

Coupling Transducers for Magneto-Inductive Waveguides

R.R.A. Syms, L. Solymar

EEE Dept., Imperial College London, Exhibition Road, London SW7 2AZ, UK
FAX +44-207-594-6308 Email r.syms@imperial.ac.uk

Abstract

A new design of resonant coupling transducer that can connect a magneto-inductive waveguide to real impedance is demonstrated. The transducer can provide exact impedance matching at two separate frequencies and approximate matching between, allowing low reflectivity to be achieved over a broad band. The theory is confirmed experimentally using thin-film magneto-inductive cable operating near 100 MHz frequency.

1. Introduction

Magneto-inductive (MI) waveguides are linear periodic structures formed from a set of magnetically coupled L-C resonators as shown in Fig. 1a [1-3]. In the loss-less case, the dispersion equation is:

$$1 - \omega_0^2/\omega^2 + \kappa \cos(ka) = 0 \quad (1)$$

Here $\omega_0^2 = 1/LC$ defines the resonant frequency and $\kappa = 2M/L$ is the coupling coefficient, where M is the mutual inductance, and ka is the phase shift per element. A MI waveguide may be terminated by inserting into the final element the characteristic impedance Z_0 as shown in Fig. 1b, where [1, 2]:

$$Z_0 = j\omega M \exp(-jka) \quad (2)$$

At mid-band ($\omega = \omega_0$, $ka = \pi/2$), Z_0 has the real value $\omega_0 M$. Although Eqn. 2 is mathematically simple, a MI waveguide cannot be matched to a real load in practice using a simple arrangement of physical components, since ka depends on frequency according to Eqn. 1. Consequently it is difficult to provide an effective method of connecting magneto-inductive and conventional RF systems without large reflections. The aim of this work is to provide a simple broadband coupling transducer.

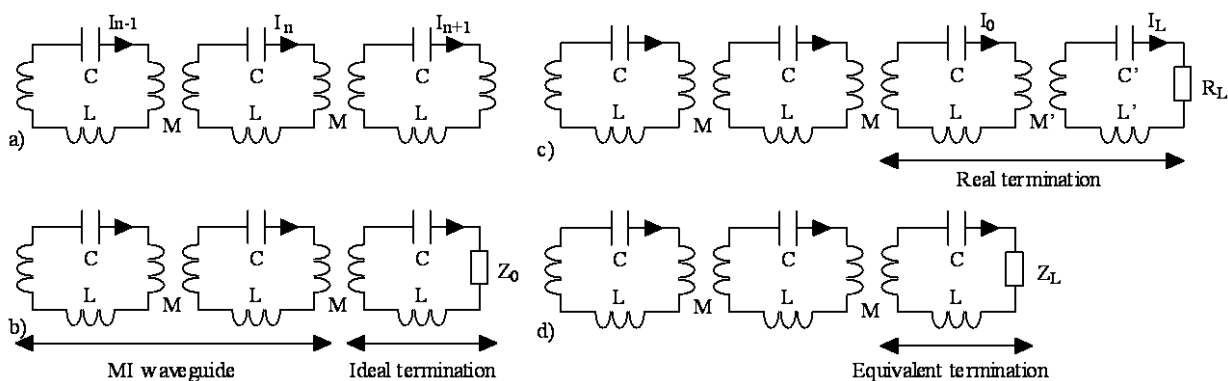


Fig. 1 a) MI waveguide, b) ideal termination, c) real termination and d) its equivalent.

2. Theory

Fig. 1c shows one obvious arrangement for connecting to a real load R_L , using a resonant circuit containing an arbitrary inductance L' and capacitance C' . The resonant circuit is coupled to the final element of the MI waveguide via a mutual inductance M' . This arrangement effectively inserts impedance

Z_L into the final element as shown in Fig. 1d, where:

$$Z_L = \omega^2 M'^2 / \{R_L + j\omega L'(1 - \omega_0'^2/\omega^2)\} \quad (3)$$

Clearly, if Z_L could be made equal to Z_0 , the transducer would provide the desired match. More generally, however, a reflection will occur. The reflection and transmission coefficients are:

$$\Gamma = -\{Z_L - Z_0\} / \{Z_L + Z_0^*\} \quad T = 2\text{Re}(Z_0) / \{Z_L + Z_0^*\} \quad (4)$$

These coefficients satisfy the power conservation relation:

$$\Gamma\Gamma^* + TT^* \text{Re}(Z_L) / \text{Re}(Z_0) = 1 \quad (5)$$

Different terminations can be compared by plotting the frequency variation of the scattering parameter $S_{11} \approx 10 \log_{10}\{|\Gamma|^2\}$. Fig. 2 shows results obtained assuming that $R_L = \omega_0 M$, $M' = M$ and $\kappa = 0.6$. Fig. 2a shows results for non-resonant terminations. Generally the matching is poor, and a reasonable match can only be made near mid-band when L'/L is unrealistically small. Fig. 2b shows results for resonant terminations, assuming in addition that the final loop is resonant at the same frequency as the elements comprising the line. For the 'obvious' choice of parameters ($L'/L = 1$), there is now a single exact null in reflectivity when $\omega = \omega_0$, providing a narrow-band impedance match. However, for a less obvious choice ($L'/L = 0.5$), there are two nulls, with low reflectivity between, providing a broadband match. Consequently, this transducer can outperform the other configurations described above, by a very considerable margin, and is easily realised using a small number of passive components.

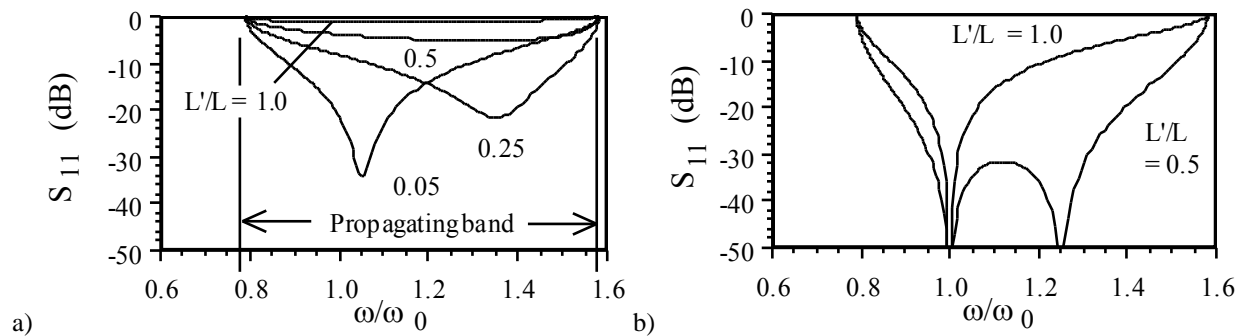


Fig. 2 Frequency variation of S_{11} for a) non-resonant and b) resonant terminations.

It is simple to show that this advantageous result is obtained because the effective impedance Z_L provides an exact match to the real and imaginary parts of the characteristic impedance Z_0 at the two frequencies $\omega = \omega_0$ and $\omega = \omega_0/\sqrt{1 - \kappa^2}$. This conclusion is confirmed in Fig. 3, which shows the frequency variations of the normalised impedance $Z_{0N} = Z_0/\omega_0 M$ and $Z_{LN} = Z_L/\omega_0 M$, again calculated assuming that $\kappa = 0.6$.

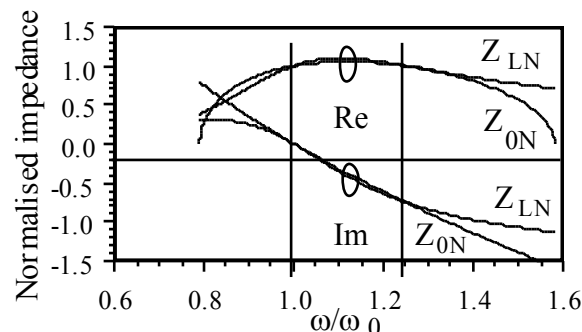


Fig. 3 Frequency variation of normalised impedances for broadband coupling transducer.

3. Experimental verification

Experimental verification was carried out using low-loss thin-film MI cables, formed by double-sided patterning of a Cu-Kapton-Cu trilayer with the unit cell of Fig. 4a [4]. Here each resonant element is 20 cm long and 4.7 mm wide and contains two single-turn inductors $L/2$ (arranged in series) and two parallel-plate capacitors $2C$ (also in series) that use the Kapton substrate as an interlayer dielectric. Cables were fabricated in 2 metre lengths using Cu and Kapton thicknesses of $35\ \mu\text{m}$ and $25\ \mu\text{m}$, and the lengths of the inductors and capacitors were varied in an array as shown in Fig. 4b. Each cable therefore contained 19 resonant elements, together with additional non-resonant transducers, which are half an element long and hence have the optimum inductance $L/2$.

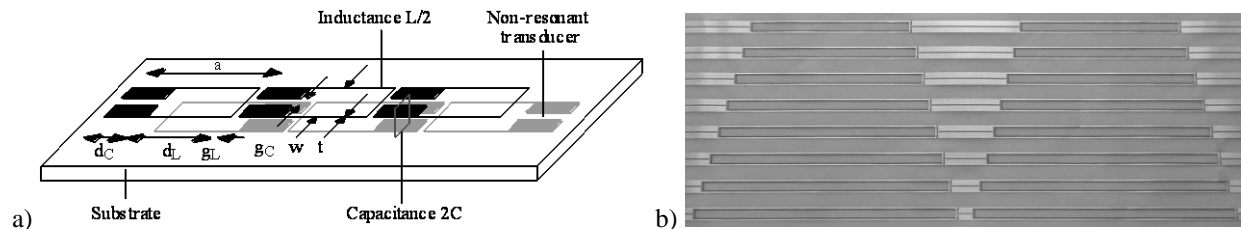


Fig. 4 Thin-film magneto-inductive cable: a) unit cell, and b) experimental realisation.

A cable with mid-band impedance close to $50\ \Omega$ ($48.6\ \Omega$) near 100 MHz frequency was identified, and its performance was measured firstly with non-resonant transducers and secondly with transducers made resonant with surface mount capacitors. Fig. 5 shows the frequency variation of S_{11} and S_{21} measured in each case, with both ends of the line connected to a network analyser. Using non-resonant transducers, the reflection is generally high. Using resonant transducers, overall transmission is considerably improved (to a maximum of $-5\ \text{dB}$) and multiple reflections are largely suppressed over the entire operating band.

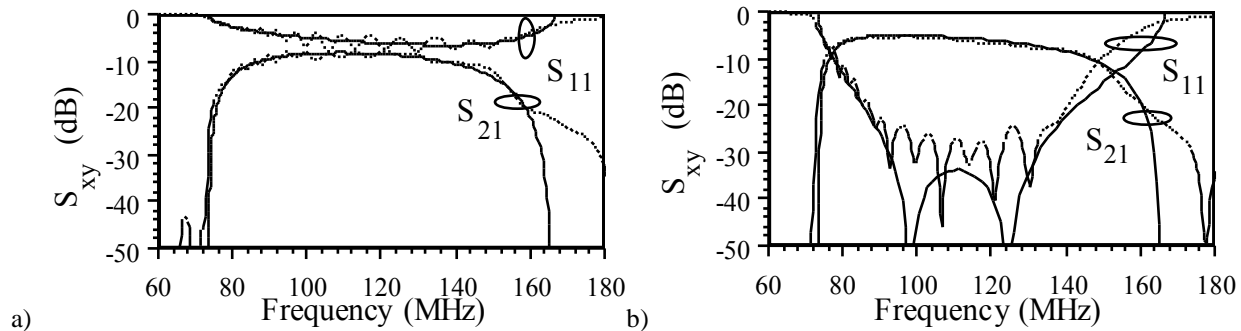


Fig. 5 Frequency variation of S_{11} and S_{21} for 2 metre MI cable with a) non-resonant and b) resonant transducers.

4. Conclusions

A simple resonant transducer capable of coupling a magneto-inductive waveguide to a real load with low reflection over a broad band has been demonstrated. The ability to connect to conventional RF systems should take magneto-inductive devices one step closer to real-world applications.

References

- [1] Shamonina E., Kalinin V.A., Ringhofer K.H., Solymar L. "Magneto-inductive waveguide" *Elect. Lett.* Vol. 38, pp 371-373, 2002
- [2] Wiltshire M.C.K., Shamonina E., Young I.R., Solymar L. "Dispersion characteristics of magneto-inductive waves: comparison between theory and experiment" *Elect. Lett.* Vol. 39, 215-217, 2003
- [3] Syms R.R.A., Young I.R., Solymar L. "Low loss magneto-inductive waveguides" *J. Phys. D. Appl. Phys.* Vol. 39, pp 3945-3951, 2006
- [4] Syms R.R.A., Young I.R., Solymar L., Floume T. "Thin-film magneto-inductive waveguides" *J. Phys. D. Appl. Phys.* Vol. 43, art 055102, 2010